Superradiant transfer of quantized orbital angular momentum between light and atoms in a ring trap

N. Piovella

Dipartimento di Fisica "Aldo Pontremoli", Università degli Studi di Milano, Via Celoria 16, I-20133 Milano, Italy

G.R.M. Robb

SUPA and Department of Physics, University of Strathclyde,Glasgow G4 0NG, Scotland, UK

R. Bachelard

Université Côte d'Azur, CNRS, Institut de Physique de Nice, 06560 Valbonne, France and
Instituto de Física de São Carlos, Universidade de São Paulo, 13560-970 São Carlos, SP, Brazil

(Dated: July 14, 2022)

The orbital angular momentum (OAM) from a laser beam can be coherently transferred to a Bose-Einstein condensate in a ring trap, in quantized units of $\hbar$. The light-matter coupling allows for the superradiant transfer of the atoms between the discrete OAM states. Tuning the ring parameters and winding number of the pump light, specific angular momentum states can be populated. This in turn allows control of the emission to generate light with OAM different from that of the pump, as the atomic ring imprints its contribution on the scattered light.

Introduction – Photons possess both translational and spin-angular momentum, where the latter is associated with different polarization states of the light wave [1]. Light may also be prepared in states with well-defined orbital angular momentum (OAM), such as in Laguerre-Gaussian (LG) beams [2]. Coherent control of the interaction between light and matter facilitates the macroscopic transfer of those quantities from one medium to another, opening up exciting and novel possibilities for quantum information engineering, such as storing and transferring light in ensembles of atoms [3].

The spatial modes of the matter field possessing orbital angular momentum are associated with a discrete infinite-dimensional (because of the quantization of the OAM) Hilbert space. Transferring orbital angular momentum from light to a Bose-Einstein condensate provides a route to entanglement that involves many orthogonal quantum states, rather than just two [4, 5]. Multi-dimensional entangled states could be of considerable importance in the field of quantum information, enabling, for example, a more efficient use of communication channels in quantum cryptography [6].

Recently, it has been shown that cold atoms trapped in a ring trap and driven by a laser beam carrying OAM are set in rotation and acquire bunching in phase [7]. Depending on the pump winding number ℓ and on the ring radius, different harmonics of the phase become bunched, similarly to the longitudinal configuration of light-matter instabilities [8]. However, a classical treatment of the azimuthal motion of the atoms means that their OAM is not quantized.

We here investigate the collective coupling between the ring of atoms and light within a quantized approach, so the OAM of the trapped condensate evolves through states with integer numbers of $\hbar$. The light-mediated dipole-dipole interactions between the atoms results in a "superradiant" coupling with the light, in analogy with the coupling achieved in cigar-shaped matter waves and linear-momenta states [9], yet here promoting the transfer of the atoms toward different OAM states. The nonlinear nature of this light-atom dynamics leads to the population of higher OAM states for the atoms and, consequently, for the scattered photons. This population of higher OAM states stems from the presence of higher harmonics in the potential experienced by the atoms. We show that this in turn enables the creation of cat states and the emission of light with OAM different from the pump.

Modelling the light-atom interaction – Let us consider that the atoms are driven resonantly by an OAM laser beam in the mode $LG_{0\ell}$, with electric field

$$E_0(\rho, \phi, z) = A_0 R(\rho) e^{i(k_0 z + \ell\phi - \omega_0 t)} + \text{c.c.}, \qquad (1)$$

with $R(\rho) = (\sqrt{2}\rho/w)^\ell \exp(-\rho^2/w^2)$ using cylindrical coordinates, w the beam waist and ℓ the pump winding number. The atoms rotate in a ring trap in the plane perpendicular to the pump propagation axis z (see Fig. 1a), and they are described by the matter wave function $\Psi(\phi, \tau)$, where ϕ refers to the azimuthal angle. Their dynamics is given by [7, 10]

$$i\frac{\partial\Psi(\phi,\tau)}{\partial\tau} = -\frac{\partial^2\Psi(\phi,\tau)}{\partial\phi^2}$$
$$+ \frac{\gamma}{2}\int_0^{2\pi} d\phi' V(\phi - \phi')|\Psi(\phi',\tau)|^2\Psi(\phi,\tau), (2)$$

with $\tau = \omega_\phi t$ the dimensionless time, $\omega_\phi = \hbar/2M\rho^2$ the angular recoil frequency, M the atom mass and ρ the ring radius. The light-atom coupling is characterized by the parameter $\gamma = N(\Gamma/\omega_\phi)(\Omega_0/2\Delta_0)^2 R^2(\rho)$, where N is the atom number, $\Omega_0 = dA_0/\hbar$ the pump Rabi frequency, Γ the atomic decay rate for the two-level transition at frequency ω_a, d the associated dipole moment, and $\Delta_0 =$

$\omega_a - \omega_0$ the pump-atom detuning. The potential V reads

$$V(\varphi) = -\frac{\cos[2k_0\rho q(\varphi) - \ell\varphi]}{k_0\rho q(\varphi)}, \quad (3)$$

where $q(\varphi) = \sqrt{\sin^2(\varphi/2) + \epsilon^2}$ and ϵ is a cut-off parameter. The potential V has a finite range due to the multimode emission in vacuum [11], and it decreases as $1/r_{jm}$ with the distance r_{jm} between the pair of atoms (j, m). Since the atoms are set on a ring of radius ρ, we have $r_{jm} = 2\rho|\sin[(\phi_j - \phi_m)/2]|$. The phenomenological cut-off ϵ in $q(\phi_j - \phi_m)$ has been added to avoid the singularity in the denominator and can be chosen arbitrarily small.

The wave function Ψ describes the atoms in a BEC state, with the normalization condition $\int_0^{2\pi} |\Psi(\phi, \tau)|^2 d\phi = 1$. This wave-function can be expanded on the basis of the angular momentum states $|m\rangle$ as $\Psi(\phi, \tau) = (1/\sqrt{2\pi}) \sum_m c_m(\tau) \exp(im\phi)$, while the potential is expanded as a Fourier series: $V(\varphi) = \sum_k V_k \exp(ik\varphi)$, with $V_k = (1/2\pi) \int_0^{2\pi} V(\varphi) \exp(-ik\varphi) d\varphi$. By projecting Eq. (2) on the state $|m\rangle$, we obtain the dynamical equations for the probability amplitudes $c_m(\tau)$:

$$\frac{dc_m}{d\tau} = -im^2 c_m - i\frac{\gamma}{2} \sum_k V_k c_{m-k} \sum_n c_{n-k}^* c_n, \quad (4)$$

where the normalization condition now reads $\sum_m |c_m(\tau)|^2 = 1$. The radiated intensity emitted by the atoms is $I(\theta, \phi) = I_1 R^2(\rho) N^2 |M(\theta, \phi)|^2$, where [10]

$$M(\theta, \phi) = \int_0^{2\pi} e^{-ik_0\rho\sin\theta\cos(\phi-\phi')+i\ell\phi'} |\Psi(\phi')|^2 \frac{d\phi'}{2\pi} (5)$$

is the dimensionless electric field, θ is the polar angle, $I_1 = (\hbar\omega_0\Gamma/8\pi r^2)(\Omega_0/2\Delta_0)^2$ and r is the distance from the detector. Introducing the m-th azimuthal bunching coefficient

$$\Phi_m(\tau) = \sum_{n=-\infty}^{+\infty} c_{n-m}^*(\tau) c_n(\tau), \quad (6)$$

the electric field rewrites as the sum of different OAM components, composed by photons with angular momentum $\hbar\ell' = \hbar(\ell + m)$:

$$M(\theta, \phi) = \sum_m (-i)^{\ell+m} J_{\ell+m}(k_0\rho\sin\theta) \Phi_m(\tau) e^{i(\ell+m)\phi}, \quad (7)$$

where $J_n(x)$ is the Bessel function of the first kind and of order n. The rescaled intensity averaged over the azimuthal angle is $\bar{I}(\theta) = \sum_m J_{\ell+m}^2(k_0\rho\sin\theta)|\Phi_m|^2$.

Linear stability analysis – Let us now discuss the atom dynamics. We observe that the cubic nonlinearity in Eq. (4) couples state m with the states $m \pm k$ provided that a k-th Fourier component V_k of the potential and a k-th azimuthal bunching Φ_k are present. More quantitatively, the dynamical growth of the azimuthal bunching
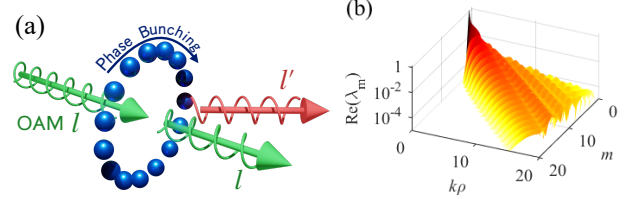

FIG. 1. (a) Scheme of the atomic ring pumped with OAM light, so the atoms acquire phase bunching. (b) Growth rate $|\text{Re}(\lambda_m)|$ for the modes m, as a function of the ring radius $k_0\rho$. The mode with the strongest rate corresponds to $m \approx k\rho$. Simulations realized with $\gamma = 0.2$ and $\epsilon = 0.1$.

at harmonic m is obtained by a linear stability analysis of Eq. (4) around the equilibrium point $\Phi_m^{(0)} = \delta_{m,0}$, which describes uniformly distributed phases. This leads to the complex eigenvalues [10]

$$\lambda_m = \pm im\sqrt{m^2 + \gamma V_m}, \quad (8)$$

where the m-th azimuthal bunching Φ_m grows exponentially as $\exp[\text{Re}(\lambda_m)\tau]$. Hence, the exponential growth of the azimuthal bunching Φ_m requires a finite imaginary part of the m-th Fourier component of the potential, V_m. For $\ell = 0$ the potential $V(\varphi)$ is an even function of φ and V_m is real, hence the system is unstable only in presence of OAM light, with $\ell \neq 0$. Intuitively, the OAM pump exerts on the atoms a torque forcing them to rotate. Since the atomic angular momentum is quantized, the atoms rotate with a discrete angular momentum, whose value is determined by the anharmonicity of the potential V.

When uniformly distributed in phase, all the atoms rotate with the same angular velocity and no macroscopic rotation is visible. However, in presence of an OAM beam, the combined effect of the pump and scattered beam creates a self-consistent potential which modulates the azimuthal atomic phases. As a result, atoms are coupled by the scattered photons, recoiling in phase as angular momentum is transferred from the light. Because the beam-matter coupling grows with the bunching in phase, an instability develops and both the bunching in phase and the scattered intensity grow exponentially until the moment when the atoms are transferred to a new OAM state $|m\rangle$. In the case of a subwavelength trap, the ring of atoms essentially behaves as a point-like dipole and the matter is transferred to the state $|\ell\rangle$, where $\hbar\ell$ is the angular momentum of the pump photons. However, increasing the ring radius ρ, the potential presents higher harmonics and is able to transfer the atoms to OAM states with m larger than ℓ.

According to Eq. (8), the system admits two different regimes: a *classical regime* when $\gamma|V_m| \gg m^2$ and thus $\lambda_m \approx \pm im\sqrt{\gamma V_m}$, which is characterized by an exponential growth rate proportional to $\sqrt{N}$, and a *quantum regime*, when $\gamma|V_m| \ll m^2$ so that $\lambda_m \approx \pm i(m^2 + \gamma V_m/2)$, which presents a rate proportional to N [12]. In the classical regime, both the states $|m\rangle$ and $|-m\rangle$ become populated almost simultaneously. Differently, in
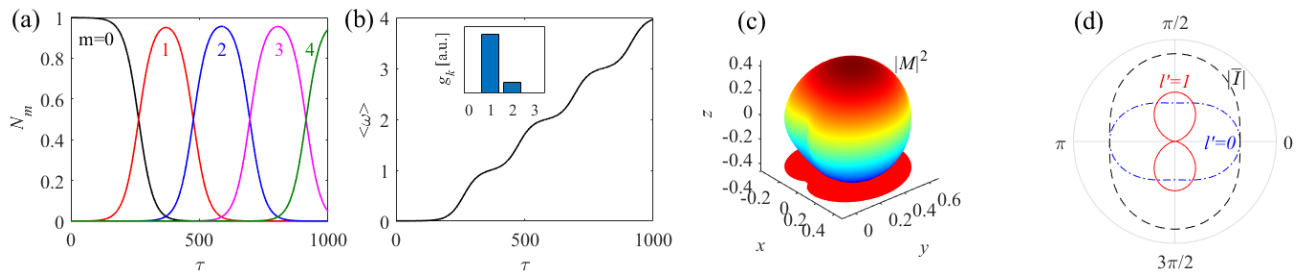
FIG. 2. (a) Populations N_m and (b) average angular velocity $\langle\omega\rangle$, in units of ω_ϕ, as a function of the dimensionless time τ. (c) Dimensionless scattered intensity $|M(\theta,\phi)|^2$ and (d) $\bar{I}(\theta)$ vs θ for $k_0\rho = 1$, $\ell = 1$ and $\gamma = 0.05$; The blue line is the component with $\ell' = 0$, the red line is the component with $\ell' = 1$ and the dashed black line is the total intensity. for $\gamma = 0.05$, $k_0\rho = 1$ and $\ell = 1$. The inset in (b) presents the rate coefficients g_k (in a.u.) as a function of k, showing that the dominant transition is for $k = 1$.

the quantum regime, the dynamical term $\exp(\pm im^2\tau)$ corresponds to a phase shift proportional to the rotational energy $L_z^2/2M\rho^2 = \hbar\omega_\phi m^2$, with orbital angular momentum $L_z = \hbar m$. This energy shift, which stems from energy and angular momentum conservation in the photon-atom scattering process, hinders the occupation of one of the two states $|\pm m\rangle$ (which one is populated depends on the sign of $\mathrm{Im}(V_m)$). This leads to the scaling of the growth rate as N for the quantum regime [12].

The scattering of the pump light into different OAM states can be deduced from the eigenspectrum, whose real part $|\mathrm{Re}(\lambda_m)|$ is presented in Fig. 1b for the quantum regime ($\gamma = 0.2$), as a function of the radius $k_0\rho$ and of m. The fact that for increasing $k_0\rho$ the maximum occurs at values of m which scales linearly with $k_0\rho$ implies that larger ring are able to populate higher OAM states of the condensate. This is a notable difference with the case of the one-dimensional quantum collective atomic recoil lasing (CARL) [8, 13, 14], where only transitions between adjacent linear momentum states are possible. This is due to the fact that CARL is characterized by a sinusoidal potential at the light wavelength, which results from the interference between the pump and the backward scattered modes. In the ring trap, the presence of higher harmonics in potential (3) allows the atoms to bunch at higher OAM states but also, as we shall see later, to scatter photons of different OAM in different directions.

Rate equations – In the quantum regime, when $\gamma|V_m| \ll m^2$, the atoms are transferred to OAM states $|m\rangle$ through a superradiant cascade which involves, essentially, only two states at the time. Then, Eqs. (4) are approximated by the following rate equations for the state populations $N_m = |c_m|^2$:

$$\frac{dN_m}{d\tau} = \left[\sum_{k=1}^{m} g_k N_{m-k} - \sum_{k=1}^{+\infty} g_k N_{m+k}\right] N_m, \qquad (9)$$

where $g_k = \gamma|\mathrm{Im}(V_k)|$ are the rate coefficients, and with the normalization condition $\sum_m N_m = 1$. These coupled equations generalize the superradiant transition between two states N_0 and N_k when only a single coefficient g_k is

present, and it solves as $N_{0,k}(\tau) = (1/2)\{1\mp\tanh[g_k(\tau - \tau_0)/2]\}$, with $\tau_0 = (1/g_k)\ln[2/\sqrt{N_k(0)}]$ the delay time. In the superradiant cascade the coherence of the matter wave function is preserved and the phases of the complex amplitudes $c_m = \sqrt{N_m}e^{i\phi_m}$ are determined by the equations

$$\frac{d\phi_m}{d\tau} = -(m^2 + \gamma V_0) - \left[\sum_{k=1}^{m} \alpha_k N_{m-k} + \sum_{k=1}^{+\infty} \alpha_k N_{m+k}\right],$$
$$(10)$$

with $\alpha_k = (\gamma/2)\mathrm{Re}(V_k)$.

For a small ring radius, $k_0\rho \ll 1$, the atoms are transferred sequentially through the OAM states by steps of $\Delta m = \ell$. This is illustrated in Fig. 2, which depicts the temporal evolution of the populations N_m for the first OAM states (see panel (a)) and the average angular velocity $\langle\omega\rangle = \sum_m m N_m$ (see panel (b)). The angular distribution of the scattered field intensity $|M(\theta,\phi)|^2$ is plotted in Fig. 2(c) at the time when the bunching is maximum ($|\Phi_1| \approx 1/2$), while panel (d) shows the total average intensity $\bar{I}(\theta)$ as a function of the polar angle θ (dashed line), together with the main OAM components. In this case the field (5) is approximated by $M(\theta,\phi) \approx -iJ_1(k_0\rho\sin\theta)\exp(i\phi) + \Phi_1^* J_0(k_0\rho\sin\theta)$, with $|\Phi_1| \approx 1/2$ and where we have neglected the term proportional to $J_2(\sin\theta)$. The average intensity is $\bar{I}(\theta) \approx J_1^2(k_0\rho\sin\theta) + |\Phi_1|^2 J_0^2(k_0\rho\sin\theta)$. In Fig. 2 we can observe the component $\ell' = 1$ (red line), the component $\ell' = 0$ (blue line) and the total intensity (dashed black line). The light with the same orbital angular momentum of the pump $\ell = 1$ is emitted in the perpendicular direction, whereas the light with $\ell = 0$ is emitted forward and backward within a large diffraction angle. The total intensity is almost isotropic, as expected for a small ring.

Populating higher OAM states – Atomic rings larger than the wavelength are able to populate directly atomic states with large OAM, taking advantage of the higher harmonics of the potential V. In Fig. 3 we illustrate how by choosing parameters such that the potential favors the coupling to several higher OAM states, the system can be cast in a macroscopic superposition. The pump with $\ell = 2$ transfers most of the atomic population from
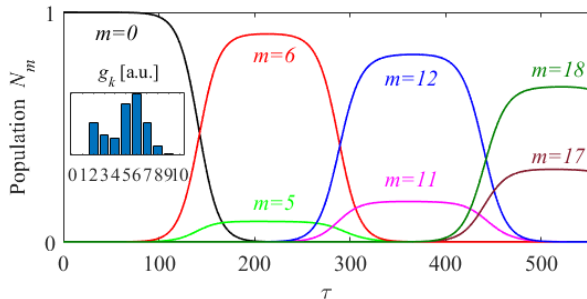
FIG. 3. Populations N_m as a function of the dimensionless time τ. Simulations realized for $k_0\rho = 5.605$, $\ell = 2$ and $\gamma = 1$. The inset presents the rate coefficients g_k (in a.u.) as a function of k, showing that the dominant transitions are for $k = 5$ and $k = 6$.

$m = 0$ to $m = 6$, and to $m = 5$ to a lesser extent, due to the set of coefficients g_k among which g_6 and g_5 are highest (the parameters have been chosen so $g_1 = 0$, so transitions with $\Delta m = 1$ are suppressed). The first transition sees a transfer of population from $m = 0$ to $m = 6$ ($N_6 = 91\%$) and to $m = 5$ ($N_5 = 9\%$). During the next transitions, the atoms are transferred to $m = 12$ and $m = 11$, then to $m = 18$ and $m = 17$, and so on, since the specific set of parameters favors transitions with $\Delta m = 6$. Thus, after two transition channels are open (that is, with $\Delta m = 5$ and 6), a macroscopic superposition of two rotational states, is created. Throughout the successive transitions toward higher phase bunching states, superpositions of two states persist. The possibility that these superposition states are Schrodinger cat states will be investigated elsewhere.

Tailoring the light emission – The dynamical evolution to higher OAM atomic states in turn results in the emission of light whose angular momentum differs from the pump one. This can be a tool either for reading the atomic state, or for producing light with a specific OAM. In particular, one may choose the ring radius such that no photons with the same OAM of the pump are emitted in a particular direction, so light with a different OAM can be collected more efficiently. As an example, we show in Fig. 4(a) how an atomic ring with radius $k_0\rho = 5$, along with a pump of winding number $\ell = 2$, is transferred to the OAM state $m = 5$.

This bunching in phase leads to five-lobe radiation pattern in the azimuthal direction, see panel (b). Because the Bessel function $J_2(k_0\rho\sin\theta)$ vanishes for $k_0\rho = 5$ and $\theta = \pi/2$, no photons with $\ell' = \ell = 2$ are emitted in the transverse direction. At this angle, only the component with $\ell' = l + m = -3$ of the scattered light is present. Thus, in this specific direction, light with a well-defined OAM, which is different from that of the pump, can be collected.

In conclusion, we have demonstrated how orbital angular momentum can be transferred coherently from a single Laguerre-Gaussian to a Bose-Einstein condensate in a ring trap. The spontaneous formation of the azimuthal bunching of ultracold atoms in the ring trap is at the core of the process. The process is similar to the quantum regime of collective atomic recoil lasing [8, 13, 14] and to the superradiant Rayleigh scattering [9], but with transfer of orbital angular momentum in units of $\hbar$ instead of linear momentum in units of $\hbar k$. Differently from these linear configurations, the many harmonics of the potential here allow to promote the atoms to one or more higher OAM states. This mechanism is particularly promising for the creation of states of matter with tailored OAM [15–17]: in the present scheme, the choice of the ring radius, by tuning the trap frequencies, allows one to manipulate the relative populations of different angular momentum states. The emission of photons with angular momentum different from that of the pump and with a specific spatial pattern offers the possibility to either use this light to read the atomic state, or to use the atomic ring to produce light with a new OAM. The atomic ring may also be used as a beam splitter, dividing the light into two or more topological states, so robust phase qubits can be generated. In this context, one may take advantage of the complete orthonormal basis formed by the OAM states to design more elaborate quantum states for quantum information processing [18].

The proposed setup correspond to ring traps with radii of a few optical wavelengths, or subwavelength for the case $\rho < \lambda$ (yet this latter case does not produce efficiently higher OAM light). Recent advances in the control of quantum gases have seen the development of atom ring traps formed from both magnetic and optical dipole potential, and more recent implementations using hybrids of both, down to $\rho = 9\mu m$ ring traps [19, 20]. Although much more challenging, nanometer-scale traps are also currently under investigation [21].

ACKNOWLEDGMENTS

[1] R. A. Beth, Direct detection of the angular momentum of light, Phys. Rev. **48**, 471 (1935).

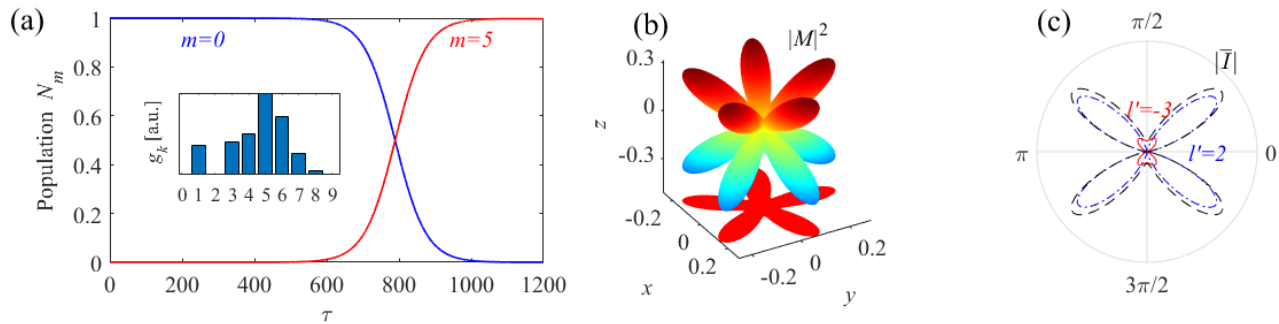[2] L. Allen, M. W. Beijersbergen, R. J. C. Spreeuw, and J. P. Woerdman, Orbital angular momentum of light

FIG. 4. (a) Population of the state $m = 0$ and $m = 5$ as a function of the dimensionless time τ. The inset shows the coefficients g_k. (b) Angular distribution of the radiation intensity $|M(\theta, \phi)|^2$, at time $\tau = 800$. (c) Dimensionless intensity $\bar{I}(\theta)$ averaged over the azimuthal angle ϕ, as a function of the polar angle θ, at time $\tau = 800$. The dashed black line stands for the total intensity, the blue line for the component $\ell' = 2$ and the red line for the component $\ell' = -3$: the latter is the only component present at $\theta = \pi/2$. Simulations realized for $k_0\rho = 5$, $\ell = 2$ and $\gamma = 0.2$.

and the transformation of laguerre-gaussian laser modes, Phys. Rev. A **45**, 8185 (1992).

[3] M. Krenn, M. Malik, M. Erhard, and A. Zeilinger, Orbital angular momentum of photons and the entanglement of laguerre–gaussian modes, Philosophical Transactions of the Royal Society A: Mathematical, Physical and Engineering Sciences **375**, 20150442 (2017).

[4] M. Andersen, C. Ryu, P. Cladé, V. Natarajan, A. Vaziri, K. Helmerson, and W. D. Phillips, Quantized rotation of atoms from photons with orbital angular momentum, Physical review letters **97**, 170406 (2006).

[5] K. Wright, L. Leslie, and N. Bigelow, Optical control of the internal and external angular momentum of a bose-einstein condensate, Physical Review A **77**, 041601 (2008).

[6] R. Fickler, G. Campbell, B. Buchler, P. K. Lam, and A. Zeilinger, Quantum entanglement of angular momentum states with quantum numbers up to 10,010, Proceedings of the National Academy of Sciences **113**, 13642 (2016).

[7] A. Gisbert, N. Piovella, G. Robb, and D. McLellan, Superradiant atomic recoil lasing with orbital-angular-momentum light, Physical Review A **105**, 023526 (2022).

[8] R. Bonifacio and L. D. S. Souza, Collective atomic recoil laser (carl) optical gain without inversion by collective atomic recoil and self-bunching of two-level atoms, Nuclear Instruments and Methods in Physics Research **341**, 360 (1994).

[9] S. Inouye, A. P. Chikkatur, D. M. Stamper-Kurn, J. Stenger, D. E. Pritchard, and W. Ketterle, Superradiant rayleigh scattering from a bose-einstein condensate, Science **285**, 571 (1999).

[10] See supplemental material at [url will be inserted by publisher] for the derivation of eqs.(2), (5) and (8)., .

[11] R. Ayllon, J. T. Mendonça, A. T. Gisbert, N. Piovella, and G. R. M. Robb, Multimode collective scattering of light in free space by a cold atomic gas, Physical Review A **100**, 023630 (2019).

[12] G. Robb, N. Piovella, and R. Bonifacio, The semiclassical and quantum regimes of super-radiant light scattering

from a bose–einstein condensate, Journal of Optics B: Quantum and Semiclassical Optics **7**, 93 (2005).

[13] N. Piovella, M. Gatelli, and R. Bonifacio, Quantum effects in the collective light scattering by coherent atomic recoil in a bose–einstein condensate, Optics Communications **194**, 167 (2001).

[14] S. Slama, S. Bux, G. Krenz, C. Zimmermann, and P. W. Courteille, Superradiant rayleigh scattering and collective atomic recoil lasing in a ring cavity, Physical Review Letters **98**, 10.1103/physrevlett.98.053603 (2007).

[15] G. Robb, Superradiant exchange of orbital angular momentum between light and cold atoms, Physical Review A **85**, 023426 (2012).

[16] P. Das, M. E. Tasgin, and Özgür E Müstecaplıoğlu, Collectively induced many-vortices topology via rotatory dicke quantum phase transition, New Journal of Physics **18**, 093022 (2016).

[17] P. Kumar, T. Biswas, K. Feliz, R. Kanamoto, M.-S. Chang, A. K. Jha, and M. Bhattacharya, Cavity optomechanical sensing and manipulation of an atomic persistent current, Physical Review Letters **127**, 113601 (2021).

[18] K. T. Kapale and J. P. Dowling, Vortex phase qubit: Generating arbitrary, counterrotating, coherent superpositions in bose-einstein condensates via optical angular momentum beams, Physical review letters **95**, 173601 (2005).

[19] L. Amico, M. Boshier, G. Birkl, A. Minguzzi, C. Miniatura, L.-C. Kwek, D. Aghamalyan, V. Ahufinger, D. Anderson, N. Andrei, *et al.*, Roadmap on atomtronics: State of the art and perspective, AVS Quantum Science **3**, 039201 (2021).

[20] S. Eckel, J. G. Lee, F. Jendrzejewski, N. Murray, C. W. Clark, C. J. Lobb, W. D. Phillips, M. Edwards, and G. K. Campbell, Hysteresis in a quantized superfluid 'atomtronic'circuit, Nature **506**, 200 (2014).

[21] R. Richberg, S. Szigeti, and A. Martin, Optical focusing of bose-einstein condensates, Physical Review A **103**, 063304 (2021).